

## On electroweak corrections to neutral current Drell-Yan

---

**Clara L. Del Pio,<sup>a,b,\*</sup> Mauro Chiesa<sup>a</sup> and Fulvio Piccinini<sup>a</sup>**

<sup>a</sup>*INFN Sezione di Pavia, Via Agostino Bassi 6, 27100 Pavia, Italy*

<sup>b</sup>*High Energy Theory Group, Department of Physics, Brookhaven National Laboratory, Upton, NY 11973, U.S.A.*

*E-mail:* [cdelpio@bnl.gov](mailto:cdelpio@bnl.gov), [mauro.chiesa@pv.infn.it](mailto:mauro.chiesa@pv.infn.it), [fulvio.piccinini@pv.infn.it](mailto:fulvio.piccinini@pv.infn.it)

Precise measurements of electroweak parameters, such as the W-boson mass and the weak mixing angle, offer an important handle for testing the Standard Model at hadronic colliders. The Drell-Yan processes, characterised by a clean experimental signature and large cross sections, are ideal for such measurements via the template-fit approach. To this aim, precise theoretical predictions obtained from Monte Carlo event generators are required. The `Z_ew-BMNNPV` code is designed for simulating the neutral-current Drell-Yan in the POWHEG-BOX framework, with NLO QCD + NLO EW accuracy and exact matching to QCD and QED parton showers. Here we comment on recent updates to the code, particularly focusing on the possibility of selecting different electroweak input-parameter and renormalization schemes. For example, choosing the weak mixing angle, in its effective or  $\overline{\text{MS}}$  definition, as an input, is critical for the high-precision determination of this parameter at hadronic colliders. We present a comparison among the predictions in different schemes and quantify the associated theoretical uncertainties.

*12th Large Hadron Collider Physics Conference (LHCP2024)*  
3-7 June 2024  
Boston, USA  
Contribution based on [1]

---

\*Speaker

## 1. Introduction

The neutral current Drell-Yan (NC DY) is a key process for the precision programme of the Large Hadron Collider (LHC), as it is characterised by a clean experimental signature and a large cross section. It can be used for detector calibration and for constraining the Parton Distribution Functions (PDFs), and it constitutes one of the irreducible background for New Physics searches at high leptonic transverse momenta and invariant masses. Moreover, it opens the possibility to perform precision tests of the Standard Model (SM) in the electroweak sector (EW), via the direct determination of electroweak parameters, like the  $W$ -boson mass [2–5] and the weak mixing angle [6–10], through the template fit method. In particular, the weak mixing angle, at difference from the  $W$  mass, can be directly determined with the NC DY without reference to other processes, either in its effective definition at the  $Z$  peak, or as a running coupling, defined in the  $\overline{\text{MS}}$  scheme, at the highest available energies [11].

The state-of-art on the experimental analysis of NC DY has reached the sub-percent precision in large regions of the dilepton phase space. This level of accuracy should find its counterpart in the theoretical calculation of DY observables. The fully-exclusive differential cross section is at present known with next-to-next-to-leading order (NNLO) accuracy in QCD [12–18] and next-to-leading order (NLO) accuracy in the electroweak sector of the Standard Model [19–31]. Recent progress has been made to include higher orders, with the calculation of inclusive  $N^3\text{LO}$  QCD corrections, the resummation of large logarithms in QCD and QED and the incorporation of multi-photon emission effects, as well as the computation of mixed  $\mathcal{O}(\alpha_s \alpha)$  NNLO corrections [32–34]. These calculations have been implemented in fixed-order simulation tools and in Monte Carlo event generators which feature a consistent matching of fixed-order calculations to parton showers, to take into account multiple soft/collinear radiations. We refer to [1] and references therein for a summary of the most recent theoretical efforts on the calculation and simulation sides.

Here we focus on the `Z_ew-BMNNPV` code [35, 36], which simulates the neutral-current Drell-Yan in the POWHEG-BOX framework [37–40] at NLO QCD + NLO EW accuracy with exact matching to QCD and QED parton showers [40, 41]. In particular, we discuss the most recent update of the code, regarding a refined treatment of EW corrections, which allows a consistent internal assessment of the theoretical uncertainties. The main novelties are the inclusion of different options for the treatment of the unstable resonance and for the handling of the hadronic contribution to the running of the electromagnetic coupling, as well as the implementation of several input-parameter and renormalization schemes. In the following we focus on the latter, presenting a description of the various input-parameter schemes and a critical comparison among the obtained predictions at the electroweak scale at fixed order in perturbation theory, considering one-loop corrections plus the class of higher-order universal fermionic terms.

## 2. Renormalization and input schemes

It is possible to divide the input-parameter schemes available in the `Z_ew-BMNNPV` code as follows.

1. The first class includes a coupling and both the  $W$  and the  $Z$  boson masses, namely  $(\alpha_i, M_W, M_Z)$  with  $\alpha_i = \alpha_0, \alpha(M_Z^2), G_\mu$ <sup>1</sup>. It is widely employed at the LHC, especially for the direct determination of  $M_W$  with the template method in charged current Drell Yan.
2. The  $(\alpha_0, G_\mu, M_Z)$  scheme features three of the most precisely-known parameters in particle physics and therefore is ideal to minimize parametric uncertainties.
3. The  $(\alpha_i, \sin \theta_{eff}^l, M_Z)$  schemes, with  $\alpha_i = \alpha_0, \alpha(M_Z^2), G_\mu$  and  $\sin \theta_{eff}^l$  as input parameter, are suitable for the precision determination of the effective weak mixing angle at the  $Z$  peak [36].

<sup>1</sup>Note that  $\alpha_0$  stands for the QED coupling constant at  $Q^2 = 0$ .

4. Lastly, the hybrid  $\overline{\text{MS}}$  scheme  $(\alpha_{\overline{\text{MS}}}(\mu), \sin^2 \theta_{\overline{\text{MS}}}(\mu^2), M_Z)$ , with the  $\overline{\text{MS}}$  couplings and the on-shell mass  $M_Z$ , can be used to probe the running of the weak mixing angle at the highest energies at LHC [11].

In each scheme, the one-loop renormalization proceeds as follows: first, one chooses three independent Lagrangian parameters in the electroweak gauge sector, which all other quantities will depend on. Next, these three parameters are related to the corresponding input quantities by means of renormalization conditions which allow to fix three counterterms. The counterterms of all derived electroweak parameters can be expressed in terms of the ones associated with the three independent quantities. Thus, in each scheme the calculation of the one-loop electroweak corrections uses different renormalization prescriptions, while the bare part of the amplitudes is formally the same, but it is evaluated with different numerical input values.

The input schemes are formally equivalent at fixed order, but can lead to numerical discrepancies in the predictions because they differ in the arrangement and consequently in the truncation of the perturbative series. The choice of one scheme over the others is thus directed by phenomenological motivations. For example, the use of  $\alpha(M_Z^2)$  or  $G_\mu$  as independent parameters allows to reabsorb in the LO prediction the large logarithms associated to the running of  $\alpha(Q^2)$  from  $Q^2 = 0$  to the electroweak scale, and thus can enable a better perturbative convergence with respect to the schemes with  $\alpha_0$  as input. On the other hand, when theoretical predictions are used to benchmark experimental results, a scheme which minimizes the parametric uncertainties stemming from the numerical input values, like  $(\alpha_0, G_\mu, M_Z)$ , is to be preferred. A third scenario is the direct determination of electroweak parameters with the template fit method, as it is done for instance with the  $W$  boson mass and the weak mixing angle. In this case, the theoretical error is part of the systematics and LO predictions could not deliver enough precision. The quantity to be measured should thus be an independent input, which can freely varied at every order in perturbation theory without affecting the accuracy of the calculation.

In the following we sketch the calculation in the different schemes, and refer to [1] for the detailed description of one-loop and NLO plus higher-order universal fermionic corrections (labelled here NLO and NLO+HO). We adopt the complex mass scheme (CMS) for the handling of the unstable gauge bosons, and use the symbol  $M_V^2$ , with  $V = W, Z$ , for the complex quantity  $\mu_V^2 = M_V^2 - i\Gamma_V M_V$ .

## 2.1 The $(\alpha_0/\alpha(M_Z^2)/G_\mu, M_W, M_Z)$ schemes

The independent parameters are the  $W$  and  $Z$  boson masses and the coupling  $\alpha_i = \alpha_0, \alpha(M_Z^2), G_\mu$ . The associated counterterms are

$$M_{Z,b}^2 = M_Z^2 + \delta M_Z^2 \quad (1)$$

$$M_{W,b}^2 = M_W^2 + \delta M_W^2 \quad (2)$$

$$e_b = e(1 + \delta Z_e), \quad (3)$$

where the subscript  $b$  indicates the bare parameter. The charge counterterm  $\delta Z_e$  is fixed by requiring that the  $\gamma e^+ e^-$  vertex does not receive radiative corrections in the Thomson limit, while  $\delta M_W^2$  and  $\delta M_Z^2$  are obtained by imposing that the gauge-boson masses are fixed to its on-shell value at all orders. The sine of the weak-mixing angle in this class of schemes is a derived quantity, defined as  $s_W^2 = 1 - M_W^2/M_Z^2$ .

If  $\alpha(M_Z^2)$  or  $G_\mu$  are in input, the charge counterterm is modified as  $\delta Z_e \rightarrow \delta Z_e - \Delta \alpha(M_Z^2)/2$  and  $\delta Z_e \rightarrow \delta Z_e - \Delta r/2$ , respectively, where  $\Delta \alpha(M_Z^2)$  takes into account the running of  $\alpha(Q^2)$  from 0 to  $M_Z^2$  and  $\Delta r$  incorporates the one-loop electroweak corrections to the muon decay in the scheme  $(\alpha_0, M_W, M_Z)$  in the Fermi theory, after subtracting the QED effects.

In these schemes the leading fermionic corrections at NLO EW, on which one wants to improve with the inclusion of higher orders, are related to

$$\delta Z_e \sim \frac{\Delta \alpha}{2}, \quad \frac{\delta s_W}{s_W} \sim \frac{1}{2} \frac{c_W^2}{s_W^2} \Delta \rho, \quad \Delta r \sim \Delta \alpha - \frac{c_W^2}{s_W^2} \Delta \rho, \quad (4)$$

where  $\Delta\rho$  contains the terms proportional to the top mass squared.

## 2.2 The $(\alpha_0/\alpha(M_Z^2)/G_\mu, \sin^2 \theta_{eff}^l, M_Z)$ schemes

In this class of schemes the sine of the effective weak mixing angle, defined from ratio of the vectorial and axial-vectorial couplings of the  $Z$  boson to the leptons as

$$\sin^2 \theta_{eff}^l \equiv \frac{I_3^l}{Q_l} \operatorname{Re} \left( \frac{-g_R^l(M_Z^2)}{g_L^l(M_Z^2) - g_R^l(M_Z^2)} \right), \quad (5)$$

is used as input parameter in place of  $M_W$ . These schemes allow the precision determination of  $\sin^2 \theta_{eff}^l$  from NC DY, by using NLO templates.

The charge and  $M_Z$  counterterms are the same as the above case, plus here we have

$$\sin^2 \theta_b = \sin^2 \theta_{eff}^l + \delta \sin^2 \theta_{eff}^l, \quad (6)$$

which is determined by imposing that the definition in Eq. (5) does not receive radiative corrections. We refer to [36] for the details of the calculation. Similarly as the class before, when  $\alpha(M_Z^2)$  or  $G_\mu$  are in input, the charge counterterm can be found from the one in the  $(\alpha_0, \sin^2 \theta_{eff}^l, M_Z)$  with the replacements  $\delta Z_e \rightarrow \delta Z_e - \Delta\alpha(M_Z^2)/2$  and  $\delta Z_e \rightarrow \delta Z_e - \Delta\tilde{r}/2$ , respectively, where  $\Delta\tilde{r}$  is the NLO electroweak corrections to the muon decay (without the QED effects in the Fermi theory) in the scheme  $(\alpha_0, \sin^2 \theta_{eff}^l, M_Z)$ .

The leading fermionic corrections in the schemes with  $\sin^2 \theta_{eff}^l$  as input parameter are associated solely to  $\delta Z_e \sim \Delta\alpha/2$  and  $\Delta\tilde{r} \sim \Delta\alpha - \Delta\rho$ , while  $\delta \sin^2 \theta_{eff}^l$  does not contain terms proportional to the logarithms of the light-fermion masses or to the top mass squared.

## 2.3 The $(\alpha_0, G_\mu, M_Z)$ scheme

In the  $(\alpha_0, G_\mu, M_Z)$  scheme, all inputs are experimentally known with high precision and the corresponding parametric uncertainties are small. The counterterms for  $e$  and  $M_Z^2$  are defined as in Sec. 2.1, while in addition we have

$$G_{\mu,b} = G_\mu + \delta G_\mu, \quad (7)$$

with  $\delta G_\mu$  fixed by requiring that the NLO corrections to the muon decay computed in the  $(\alpha_0, G_\mu, M_Z)$  scheme (after removing the QED effects in the Fermi theory) vanish. The weak mixing angle and the  $W$  boson mass are derived quantities in this scheme. Two different choices for running this scheme are available in the code: in the following, we set the optional flag `azinscheme4=1`, and thus evaluate the matrix element with the coupling  $\alpha = \alpha_0/(1 - \Delta\alpha(M_Z^2))$ , where  $\Delta\alpha(M_Z^2)$  is computed from the input  $\alpha_0$ . Deactivating this flag would imply the use of  $\alpha_0$  to calculate the amplitude.

The inclusion of higher orders is achieved by introducing a Born-improved amplitude written in terms of the effective couplings  $\alpha = \alpha_0/(1 - \Delta\alpha(M_Z^2))$  and

$$\overline{\sin^2}^{\text{HO}} \theta_{eff}^l = \frac{1}{2} - \sqrt{\frac{1}{4} - \frac{\pi\alpha}{\sqrt{2}G_\mu M_Z^2}} \left( 1 + \Delta\tilde{r}_{\text{HO}} \right), \quad (8)$$

where  $\Delta\tilde{r}_{\text{HO}}$  has the same form of  $\Delta\tilde{r}$ , defined in the schemes with  $\sin^2 \theta_{eff}^l$  as independent quantity, but it is evaluated with different numerical inputs and contains the higher-order top-mass enhanced contributions. It is understood that one should subtract the NLO expansion in  $\Delta\tilde{r}$  and  $\Delta\alpha$  to avoid the double-counting of  $\mathcal{O}(\alpha)$  corrections.

## 2.4 The $(\alpha_{\overline{\text{MS}}}, s_{W \overline{\text{MS}}}^2, M_Z)$ scheme

In the  $(\alpha_{\overline{\text{MS}}}, s_{W \overline{\text{MS}}}^2, M_Z)$  scheme, the independent parameters are the one-shell  $Z$  mass and the  $\overline{\text{MS}}$  running couplings  $\alpha_{\overline{\text{MS}}}(\mu_0^2)$  and  $s_{W \overline{\text{MS}}}^2(\mu_0^2)$  for a given  $\overline{\text{MS}}$  renormalization scale  $\mu_0$  selected by the user, which are then evolved to the chosen renormalization scale  $\mu$ , which can be either fixed or dynamical, following [42–44]. In the following we adopt the dynamical choice by setting  $\mu$  to the dilepton invariant mass. The  $Z$ -boson mass counterterm is defined as in Sec. 2.1, while we have

$$\begin{aligned} \delta Z_{e \overline{\text{MS}}}(\mu^2) = & -\frac{\alpha}{4\pi} \left\{ \sum_{f=l,q} \frac{N_C^f 2Q_f^2}{3} \left[ -\Delta_{\text{UV}} + \log \frac{\mu^2}{\mu_{\text{Dim}}^2} \right] + \frac{7}{2} \left( \Delta_{\text{UV}} - \log \frac{\mu^2}{\mu_{\text{Dim}}^2} \right) \right. \\ & \left. + \delta_{D, \text{top}} \frac{8}{9} \log \frac{M_{\text{top}}^2}{\mu^2} \theta(M_{\text{top}}^2 - \mu^2) + \delta_{D, W} \left[ -\frac{7}{2} \log \frac{M_{W, \text{thr.}}^2}{\mu^2} + \frac{1}{3} \right] \theta(M_{W, \text{thr.}}^2 - \mu^2) \right\} \end{aligned} \quad (9)$$

for the charge counterterm and

$$\frac{\delta s_{W \overline{\text{MS}}}^2(\mu^2)}{s_{W \overline{\text{MS}}}^2} = \frac{c_{W \overline{\text{MS}}}}{2s_{W \overline{\text{MS}}}} \left( \delta Z_{Z \overline{\text{MS}}} - \delta Z_{AZ \overline{\text{MS}}} \right) + \delta_{D, W} \frac{\alpha}{6\pi} \frac{c_{W \overline{\text{MS}}}^2}{s_{W \overline{\text{MS}}}^2} \theta(M_{W, \text{thr.}}^2 - \mu^2) \quad (10)$$

for the one of the weak mixing angle, where  $\delta Z_{Z \overline{\text{MS}}}$  and  $\delta Z_{AZ \overline{\text{MS}}}$  for the  $\overline{\text{MS}}$  scheme are defined in [1]. In Eqs. (9)–(10) one can recognise the top and  $W$  decoupling if  $\mu$  is smaller than the top or  $W$  mass; discontinuity effects appear at  $\mathcal{O}(\alpha)$  at the  $W$  threshold and at  $\mathcal{O}(\alpha^2)$ ,  $\mathcal{O}(\alpha\alpha_S)$ , and  $\mathcal{O}(\alpha\alpha_S^2)$  for the top one. One can choose to deactivate the decoupling with the flags `decouplemwOFF` (`decouplemtOFF`), which set  $\delta_{D, W}$  ( $\delta_{D, \text{top}}$ ) to zero, as well as the threshold corrections (`OFFthreshcorrs`). Note that, when the decoupling is enabled, the heavy degrees of freedom are integrated out in the evolution equations, but not in the calculation of the matrix element. Finally, in the  $(\alpha_{\overline{\text{MS}}}, s_{W \overline{\text{MS}}}^2, M_Z)$  scheme, as in the  $(\alpha_0, \sin^2 \theta_{eff}^l, M_Z)$  one, the universal higher-order effects are already included in the LO amplitude through the running of the couplings.

## 3. Numerical results

We now can compare the predictions for the dilepton invariant mass distribution  $d\sigma/dM_{ll}$ , obtained with the different parameter schemes, by considering the  $\mu^+ \mu^-$  final state, at  $\sqrt{s} = 13$  TeV. The only selection criterium is an invariant mass cut  $M_{ll} \geq 50$  GeV.

On the left of Fig. 1, the predictions for different inputs are plotted w.r.t to the ones obtained in the reference  $(\alpha(M_Z^2), \sin^2 \theta_{eff}^l, M_Z)$  scheme, which is free from the universal fermionic corrections, at LO (upper panel), NLO (middle panel) and NLO+HO (lower one). In the last panel we include the results in the  $\overline{\text{MS}}$  scheme. One can clearly see how the spread among the schemes is reduced from the 20% at LO to 2% at NLO and few 0.1% at NLO+HO. The behaviour of the curves can be understood by writing the corrections in each scheme in terms of a non-enhanced part, formally the same one as in the  $(\alpha(M_Z^2), \sin^2 \theta_{eff}^l, M_Z)$  scheme but with different numerical inputs, plus a shift in  $s_W^2$  and an overall effect coming from the other coupling. For instance, at LO, all schemes with  $\sin^2 \theta_{eff}^l$  as input differ from the one at denominator only for the value of the LO couplings, and the corresponding curves are thus horizontal constant shifts, while adopting  $M_W$  as input induces a shape effect due to the different value of  $s_W^2$ . At NLO+HO, the corrections are essentially written as Born-improved matrix elements with effective couplings  $\alpha$  and  $s_W^2$ , which reabsorb the leading part of the fermionic corrections up to the scale  $M_Z$  and thus reduce the spread among the predictions. The residual difference is mainly related to the bosonic corrections, which are computed at one-loop accuracy.

Some comment should be spent on the  $\overline{\text{MS}}$  scheme, which is showed by the black lines in the lower panel: the solid one corresponds to setting as inputs  $\alpha_{\overline{\text{MS}}}(M_Z^2)$  and  $s_{W \overline{\text{MS}}}^2(M_Z^2)$ , i.e. the  $\overline{\text{MS}}$  values at  $M_Z^2$

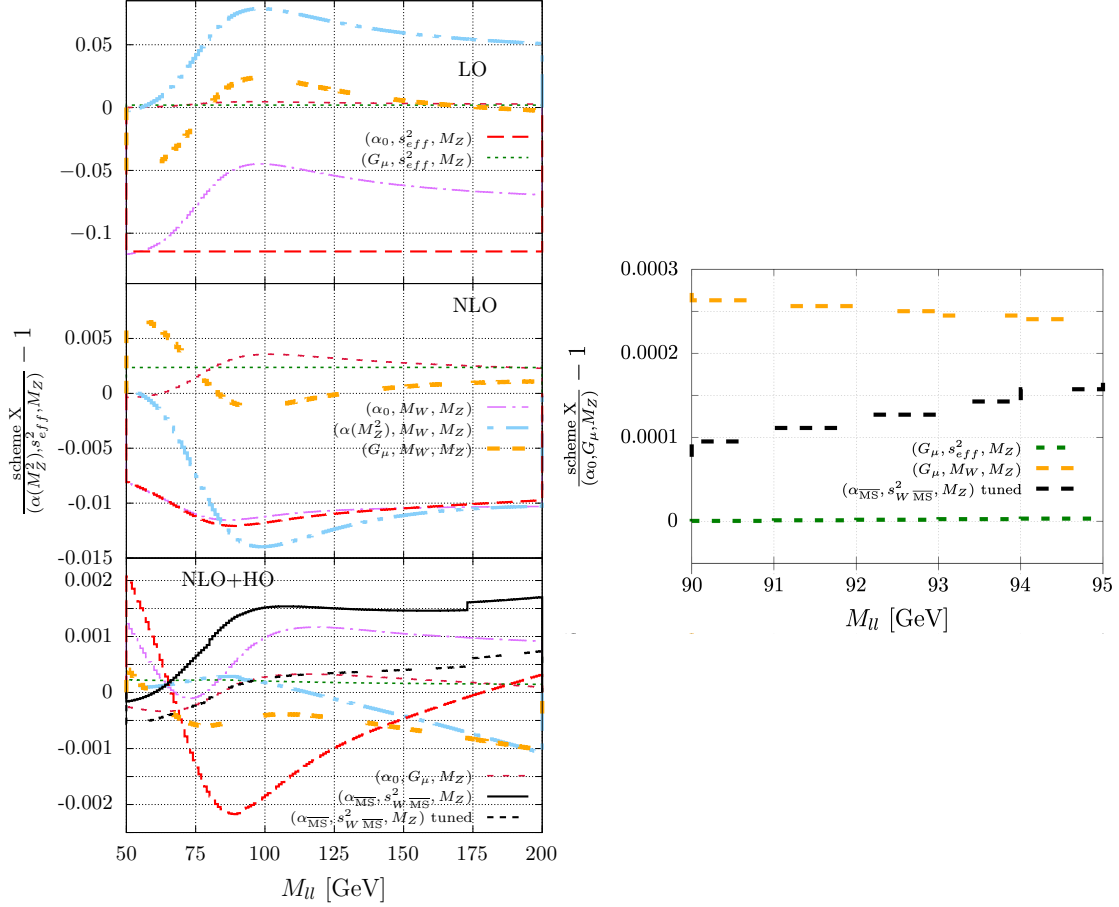


**Figure 1:** LEFT: Relative difference of the predictions for the dilepton invariant mass cross section distribution at LO (top), NLO (center), NLO+HO (bottom). RIGHT: The same as the lower panel on the left, but after performing the tuning. The calculation is performed in the pole scheme to reduce spurious  $\mathcal{O}(\alpha)$  effects due to the use of complex masses.

taked from the PDG [45], while the dashed line is obtained by computing  $\alpha_{\overline{\text{MS}}}(M_Z^2)$  and  $s_{W \overline{\text{MS}}}^2(M_Z^2)$  from their effective counterparts:

$$\alpha_{\overline{\text{MS}}}(\mu^2) = \frac{\alpha_0}{1 - \Delta\hat{\alpha}(\mu^2)}, \quad s_{W \overline{\text{MS}}}^2(M_Z^2) = \frac{1}{2} - \sqrt{\frac{1}{4} - \frac{\pi\alpha_0}{\sqrt{2}G_\mu M_Z^2(1 - \Delta\hat{\alpha}(M_Z^2))}\left(1 + \Delta r_{\overline{\text{MS}}, \text{HO}}\right)}, \quad (11)$$

where the second equation is analogous to Eq. (8). This is a first kind of tuning, as we discuss in the next section.

### 3.1 Tuning

The input schemes presented so far use genuinely independent parameters, each set to its experimental value. However, one can choose a reference scheme, for example the LEP one  $(\alpha_0, G_\mu, M_Z)$ , and use these three parameters to compute the numerical prediction for  $M_W$  and  $\sin^2 \theta_{eff}^l$ , then employed as inputs for the schemes  $(G_\mu, M_W, M_Z)$  and  $(G_\mu, \sin^2 \theta_{eff}^l, M_Z)$ , respectively. We refer to the literature produced by the LEP1 theoretical collaborations [46–59] for the tuning equations. Since the tuning is performed at the best possible accuracy (here NLO+HO), higher-order effects are effectively included in the numerical inputs

and the spread among the schemes is reduced, at least in the peak region. In fact, as it can be seen on the right of Fig. 1, the difference on the cross section reaches a maximum of 0.025%.

## 4. Conclusions

As the LHC reaches higher precision in the determination of SM parameters, in particular in the electroweak sector, EW corrections should be taken into account and properly implemented in Monte Carlo event generators. In this talk, we present the latest version of the Z\_ew-BMNNPV code and discuss how the choice of electroweak input-parameter and renormalization schemes can play an important role for the quantification of theoretical uncertainties and for the direct determination of SM parameters via the template fit method, as for the case of the weak mixing angle in both its on-shell and  $\overline{\text{MS}}$  definitions.

## References

- [1] M. Chiesa, C. L. Del Pio, and F. Piccinini *Eur. Phys. J. C* **84** no. 5, (2024) 539, [arXiv:2402.14659](https://arxiv.org/abs/2402.14659) [hep-ph].
- [2] CDF, D0 Collaboration, T. A. Aaltonen *et al.* *Phys. Rev. D* **88** no. 5, (2013) 052018, [arXiv:1307.7627](https://arxiv.org/abs/1307.7627) [hep-ex].
- [3] ATLAS Collaboration, M. Aaboud *et al.* *Eur. Phys. J. C* **78** no. 2, (2018) 110, [arXiv:1701.07240](https://arxiv.org/abs/1701.07240) [hep-ex]. [Erratum: Eur.Phys.J.C 78, 898 (2018)].
- [4] CDF Collaboration, T. Aaltonen *et al.* *Science* **376** no. 6589, (2022) 170–176.
- [5] ATLAS Collaboration, “Improved  $W$  boson Mass Measurement using 7 TeV Proton-Proton Collisions with the ATLAS Detector.” 2023.
- [6] CMS Collaboration, S. Chatrchyan *et al.* *Phys. Rev. D* **84** (2011) 112002, [arXiv:1110.2682](https://arxiv.org/abs/1110.2682) [hep-ex].
- [7] ATLAS Collaboration, G. Aad *et al.* *JHEP* **09** (2015) 049, [arXiv:1503.03709](https://arxiv.org/abs/1503.03709) [hep-ex].
- [8] LHCb Collaboration, R. Aaij *et al.* *JHEP* **11** (2015) 190, [arXiv:1509.07645](https://arxiv.org/abs/1509.07645) [hep-ex].
- [9] CDF, D0 Collaboration, T. A. Aaltonen *et al.* *Phys. Rev. D* **97** no. 11, (2018) 112007, [arXiv:1801.06283](https://arxiv.org/abs/1801.06283) [hep-ex].
- [10] CMS Collaboration, A. M. Sirunyan *et al.* *Eur. Phys. J. C* **78** no. 9, (2018) 701, [arXiv:1806.00863](https://arxiv.org/abs/1806.00863) [hep-ex].
- [11] S. Amoroso, M. Chiesa, C. L. Del Pio, K. Lipka, F. Piccinini, F. Vazzoler, and A. Vicini *Phys. Lett. B* **844** (2023) 138103, [arXiv:2302.10782](https://arxiv.org/abs/2302.10782) [hep-ph].
- [12] R. Hamberg, W. L. van Neerven, and T. Matsuura *Nucl. Phys. B* **359** (1991) 343–405. [Erratum: Nucl.Phys.B 644, 403–404 (2002)].
- [13] C. Anastasiou, L. J. Dixon, K. Melnikov, and F. Petriello *Phys. Rev. D* **69** (2004) 094008, [arXiv:hep-ph/0312266](https://arxiv.org/abs/hep-ph/0312266).
- [14] K. Melnikov and F. Petriello *Phys. Rev. D* **74** (2006) 114017, [arXiv:hep-ph/0609070](https://arxiv.org/abs/hep-ph/0609070).
- [15] K. Melnikov and F. Petriello *Phys. Rev. Lett.* **96** (2006) 231803, [arXiv:hep-ph/0603182](https://arxiv.org/abs/hep-ph/0603182).
- [16] S. Catani, L. Cieri, G. Ferrera, D. de Florian, and M. Grazzini *Phys. Rev. Lett.* **103** (2009) 082001, [arXiv:0903.2120](https://arxiv.org/abs/0903.2120) [hep-ph].
- [17] R. Gavin, Y. Li, F. Petriello, and S. Quackenbush *Comput. Phys. Commun.* **182** (2011) 2388–2403, [arXiv:1011.3540](https://arxiv.org/abs/1011.3540) [hep-ph].
- [18] R. Gavin, Y. Li, F. Petriello, and S. Quackenbush *Comput. Phys. Commun.* **184** (2013) 208–214, [arXiv:1201.5896](https://arxiv.org/abs/1201.5896) [hep-ph].
- [19] U. Baur, S. Keller, and W. K. Sakumoto *Phys. Rev. D* **57** (1998) 199–215, [arXiv:hep-ph/9707301](https://arxiv.org/abs/hep-ph/9707301).
- [20] V. A. Zykunov *Eur. Phys. J. direct* **3** no. 1, (2001) 9, [arXiv:hep-ph/0107059](https://arxiv.org/abs/hep-ph/0107059).
- [21] U. Baur, O. Brein, W. Hollik, C. Schappacher, and D. Wackerlo *Phys. Rev. D* **65** (2002) 033007, [arXiv:hep-ph/0108274](https://arxiv.org/abs/hep-ph/0108274).
- [22] S. Dittmaier and M. Krämer *Phys. Rev. D* **65** (2002) 073007, [arXiv:hep-ph/0109062](https://arxiv.org/abs/hep-ph/0109062).
- [23] U. Baur and D. Wackerlo *Phys. Rev. D* **70** (2004) 073015, [arXiv:hep-ph/0405191](https://arxiv.org/abs/hep-ph/0405191).
- [24] A. Arbuzov, D. Bardin, S. Bondarenko, P. Christova, L. Kalinovskaya, G. Nanava, and R. Sadykov *Eur. Phys. J. C* **46** (2006) 407–412, [arXiv:hep-ph/0506110](https://arxiv.org/abs/hep-ph/0506110). [Erratum: Eur.Phys.J.C 50, 505 (2007)].

[25] C. M. Carloni Calame, G. Montagna, O. Nicrosini, and A. Vicini *JHEP* **12** (2006) 016, [arXiv:hep-ph/0609170](https://arxiv.org/abs/hep-ph/0609170).

[26] V. A. Zykunov *Phys. Rev. D* **75** (2007) 073019, [arXiv:hep-ph/0509315](https://arxiv.org/abs/hep-ph/0509315).

[27] C. M. Carloni Calame, G. Montagna, O. Nicrosini, and A. Vicini *JHEP* **10** (2007) 109, [arXiv:0710.1722](https://arxiv.org/abs/0710.1722) [hep-ph].

[28] A. Arbuzov, D. Bardin, S. Bondarenko, P. Christova, L. Kalinovskaya, G. Nanava, and R. Sadykov *Eur. Phys. J. C* **54** (2008) 451–460, [arXiv:0711.0625](https://arxiv.org/abs/0711.0625) [hep-ph].

[29] S. Brensing, S. Dittmaier, M. Krämer, and A. Mück *Phys. Rev. D* **77** (2008) 073006, [arXiv:0710.3309](https://arxiv.org/abs/0710.3309) [hep-ph].

[30] S. Dittmaier and M. Huber *JHEP* **01** (2010) 060, [arXiv:0911.2329](https://arxiv.org/abs/0911.2329) [hep-ph].

[31] R. Boughezal, Y. Li, and F. Petriello *Phys. Rev. D* **89** no. 3, (2014) 034030, [arXiv:1312.3972](https://arxiv.org/abs/1312.3972) [hep-ph].

[32] T. Armadillo, R. Bonciani, S. Devoto, N. Rana, and A. Vicini [arXiv:2205.03345](https://arxiv.org/abs/2205.03345) [hep-ph].

[33] T. Armadillo, R. Bonciani, S. Devoto, N. Rana, and A. Vicini *JHEP* **05** (2022) 072, [arXiv:2201.01754](https://arxiv.org/abs/2201.01754) [hep-ph].

[34] R. Bonciani, F. Buccioni, N. Rana, and A. Vicini *JHEP* **02** (2022) 095, [arXiv:2111.12694](https://arxiv.org/abs/2111.12694) [hep-ph].

[35] L. Barze, G. Montagna, P. Nason, O. Nicrosini, F. Piccinini, and A. Vicini *Eur. Phys. J. C* **73** no. 6, (2013) 2474, [arXiv:1302.4606](https://arxiv.org/abs/1302.4606) [hep-ph].

[36] M. Chiesa, F. Piccinini, and A. Vicini *Phys. Rev. D* **100** no. 7, (2019) 071302, [arXiv:1906.11569](https://arxiv.org/abs/1906.11569) [hep-ph].

[37] P. Nason *JHEP* **11** (2004) 040, [arXiv:hep-ph/0409146](https://arxiv.org/abs/hep-ph/0409146).

[38] S. Frixione, P. Nason, and C. Oleari *JHEP* **11** (2007) 070, [arXiv:0709.2092](https://arxiv.org/abs/0709.2092) [hep-ph].

[39] S. Alioli, P. Nason, C. Oleari, and E. Re *JHEP* **06** (2010) 043, [arXiv:1002.2581](https://arxiv.org/abs/1002.2581) [hep-ph].

[40] T. Ježo and P. Nason *JHEP* **12** (2015) 065, [arXiv:1509.09071](https://arxiv.org/abs/1509.09071) [hep-ph].

[41] C. M. Carloni Calame, M. Chiesa, H. Martinez, G. Montagna, O. Nicrosini, F. Piccinini, and A. Vicini *Phys. Rev. D* **96** no. 9, (2017) 093005, [arXiv:1612.02841](https://arxiv.org/abs/1612.02841) [hep-ph].

[42] J. Erler *Phys. Rev. D* **59** (1999) 054008, [arXiv:hep-ph/9803453](https://arxiv.org/abs/hep-ph/9803453).

[43] J. Erler and M. J. Ramsey-Musolf *Phys. Rev. D* **72** (2005) 073003, [arXiv:hep-ph/0409169](https://arxiv.org/abs/hep-ph/0409169).

[44] J. Erler and R. Ferro-Hernández *JHEP* **03** (2018) 196, [arXiv:1712.09146](https://arxiv.org/abs/1712.09146) [hep-ph].

[45] Particle Data Group Collaboration, R. L. Workman *PTEP* **2022** (2022) 083C01.

[46] W. F. L. Hollik *Fortsch. Phys.* **38** (1990) 165–260.

[47] M. Consoli, W. Hollik, and F. Jegerlehner, “Electroweak Radiative Corrections for  $Z$  Physics,” in *LEP Physics Workshop*. 9, 1989.

[48] G. Burgers and F. Jegerlehner *Conf. Proc. C* **8902201** (1989) 55–88.

[49] G. Altarelli, R. Kleiss, and C. Verzegnassi, eds., *Z Physics at LEP-1. Proceedings, Workshop, Geneva, Switzerland, September 4-5, 1989. Vol. 1: Standard Physics*, CERN Yellow Reports: Conference Proceedings. 9, 1989.

[50] D. Y. Bardin, M. S. Bilenky, A. Chizhov, A. Sazonov, O. Fedorenko, T. Riemann, and M. Sachwitz *Nucl. Phys. B* **351** (1991) 1–48, [arXiv:hep-ph/9801208](https://arxiv.org/abs/hep-ph/9801208).

[51] D. Y. Bardin, M. S. Bilenky, A. Sazonov, Y. Sedykh, T. Riemann, and M. Sachwitz *Phys. Lett. B* **255** (1991) 290–296, [arXiv:hep-ph/9801209](https://arxiv.org/abs/hep-ph/9801209).

[52] D. Y. Bardin, W. Hollik, and T. Riemann *Z. Phys. C* **49** (1991) 485–490.

[53] D. Y. Bardin *et al.* [arXiv:hep-ph/9412201](https://arxiv.org/abs/hep-ph/9412201).

[54] D. Y. Bardin *et al.*, “Electroweak working group report,” in *Workshop Group on Precision Calculations for the Z Resonance (2nd meeting held Mar 31, 3rd meeting held Jun 13)*. 9, 1997. [arXiv:hep-ph/9709229](https://arxiv.org/abs/hep-ph/9709229).

[55] V. A. Novikov, L. B. Okun, and M. I. Vysotsky *Phys. Lett. B* **324** (1994) 89–97.

[56] V. A. Novikov, L. B. Okun, A. N. Rozanov, M. I. Vysotsky, and V. P. Yurov *Phys. Lett. B* **331** (1994) 433–440, [arXiv:hep-ph/9401338](https://arxiv.org/abs/hep-ph/9401338).

[57] V. A. Novikov, L. B. Okun, A. N. Rozanov, and M. I. Vysotsky *Mod. Phys. Lett. A* **9** (1994) 2641–2648, [arXiv:hep-ph/9404327](https://arxiv.org/abs/hep-ph/9404327).

[58] G. Montagna, F. Piccinini, O. Nicrosini, G. Passarino, and R. Pittau *Nucl. Phys. B* **401** (1993) 3–66.

[59] G. Montagna, F. Piccinini, O. Nicrosini, G. Passarino, and R. Pittau *Comput. Phys. Commun.* **76** (1993) 328–360.